

A testable radiative neutrino mass model with multi-charged particles

Kingman Cheung^{1,2,3,*} and Hiroshi Okada^{1,†}

¹*Physics Division, National Center for Theoretical Sciences, Hsinchu, Taiwan 300*

²*Department of Physics, National Tsing Hua University, Hsinchu 300, Taiwan*

³*Division of Quantum Phases and Devices, School of Physics,
Konkuk University, Seoul 143-701, Republic of Korea*

(Dated: March 7, 2024)

Abstract

We propose a radiatively-induced neutrino mass model at one-loop level by introducing a pair of doubly-charged fermions and a few multi-charged bosons. We investigate the contributions of the model to neutrino masses, lepton-flavor violations, muon $g - 2$, oblique parameters, and collider signals, and find a substantial fraction of the parameter space that can satisfy all the constraints. Furthermore, we discuss the possibility of detecting the doubly-charged fermions at the LHC.

Keywords:

*Electronic address: cheung@phys.nthu.edu.tw

†Electronic address: macokada3hiroshi@cts.nthu.edu.tw

	E	k^{++}	$\Phi_{\frac{3}{2}}$	$\Phi_{\frac{5}{2}}$
$SU(2)_L$	1	1	2	2
$U(1)_Y$	-2	2	$\frac{3}{2}$	$\frac{5}{2}$

TABLE I: Charge assignments of new fields under $SU(2)_L \times U(1)_Y$, where all these fields are singlet under $SU(3)_C$.

I. INTRODUCTION

Neutrino oscillation experiments have accumulated enough evidences that the neutrinos do have masses. Massive neutrino is one of the established evidences beyond the standard model (SM). In order to reconcile the tiny neutrino mass to the mass of other SM fermions, many different mechanisms have been proposed to explain the neutrino masses. One of the ideas that the scale of the neutrino Yukawa couplings should not be too different from the other Yukawa couplings – radiatively induced neutrino mass scenario – the neutrino is generated at loop level while the tree-level one is forbidden [1–4]. Because of loop suppression, small enough neutrino masses can be generated. At the same time, it requires new fields that run inside the loop(s) of the neutrino-mass generating diagrams. These new fields may be of interests to explain other phenomena, such as dark matter, muon anomalous magnetic moment, and/or to give interesting signatures at the Large Hadron Collider (LHC).

In this work, we propose a simple extension of the SM by introducing 3 generations of doubly-charged fermion pairs and three multi-charged bosonic fields [5]. All of them participate in generation of neutrino mass at one-loop level. We show that the model can explain the anomalous magnetic moment without conflict constraints of the lepton-flavor violating processes and oblique parameters. Also we discuss the possibility of detecting some of the new fields at the LHC.

This paper is organized as follows. In Sec. II, we review the model, describe several constraints, and show numerical results. In Sec. III, we discuss the collider signatures. We conclude in Sec. IV.

II. MODEL SETUP AND CONSTRAINTS

In the model, we introduce three families of doubly charged fermions E , and three types of new bosons k^{++} , $\Phi_{3/2}$ and $\Phi_{5/2}$, in addition to the SM fields, as shown in Table I. Under their charge assignments, the relevant Yukawa Lagrangian and the non-trivial terms of Higgs potential are given by

$$-\mathcal{L}_Y = f_{ia}\bar{L}_i P_R E_a \Phi_{3/2} + M_{E_a}\bar{E}_a E_a + \kappa_{ij}\bar{e}_i P_R e_j^c k^{--} + g_{ia}\bar{L}_i P_R E_a^c \Phi_{5/2}^* + \text{h.c.}, \quad (\text{II.1})$$

$$V = \left[\mu(H^T \cdot \Phi_{\frac{3}{2}})k^{--} + \text{c.c.} \right] + \left[\mu'(H^\dagger \Phi_{\frac{5}{2}})k^{--} + \text{c.c.} \right] \\ + \left[\lambda_0(H^T \cdot \Phi_{\frac{3}{2}})(H^T \cdot \Phi_{\frac{5}{2}}^*) + \text{c.c.} \right] + \left[\lambda'_0(\Phi_{\frac{5}{2}}^\dagger \Phi_{\frac{3}{2}})\mathbf{3}(H^T H)\mathbf{3} + \text{c.c.} \right], \quad (\text{II.2})$$

where H is the SM Higgs field that develops a nonzero vacuum expectation value (VEV), which is symbolized by $\langle H \rangle \equiv v/\sqrt{2}$, and $(i, a) = 1 - 3$ are generation indices. The f and g terms contribute to the active neutrino masses, while the κ term does not contribute to the neutrino sector but plays a role of mediating the decays of the new particles into the SM particles. In this work, all the coefficients are chosen to be real and positive for simplicity.

We parameterize the scalar fields as

$$\Phi_{\frac{3}{2}} = \begin{bmatrix} \phi_{3/2}^{++} \\ \phi_{3/2}^+ \end{bmatrix}, \quad \Phi_{\frac{5}{2}} = \begin{bmatrix} \phi_{5/2}^{+++} \\ \phi_{5/2}^{++} \end{bmatrix}, \quad (\text{II.3})$$

where the lower index in each component represents the hypercharge of the field. Due to the $\mu^{(\prime)}$ and $\lambda_0^{(\prime)}$ terms in Eq. (II.2), the three doubly-charged bosons in basis of $(k^{++}, \phi_{3/2}^{++}, \phi_{5/2}^{++})$ fully mix with one another. The mixing matrix and mass eigenstates are defined as follows:

$$\begin{bmatrix} k^{++} \\ \phi_{3/2}^{++} \\ \phi_{5/2}^{++} \end{bmatrix} = \sum_{a=1-3} O_{ia} H_a^{++}, \quad O \equiv \begin{bmatrix} 1 & 0 & 0 \\ 0 & c_{23} & s_{23} \\ 0 & -s_{23} & c_{23} \end{bmatrix} \begin{bmatrix} c_{13} & 0 & s_{13} \\ 0 & 1 & 0 \\ -s_{13} & 0 & c_{13} \end{bmatrix} \begin{bmatrix} c_{12} & s_{12} & 0 \\ -s_{12} & c_{12} & 0 \\ 0 & 1 & 0 \end{bmatrix}, \quad (\text{II.4})$$

therefore one can rewrite the Lagrangian in terms of the mass eigenstate as follows:

$$k^{++} = \sum_{a=1-3} O_{1a} H_a^{++}, \quad \phi_{3/2}^{++} = \sum_{a=1-3} O_{2a} H_a^{++}, \quad \phi_{5/2}^{++} = \sum_{a=1-3} O_{3a} H_a^{++}. \quad (\text{II.5})$$

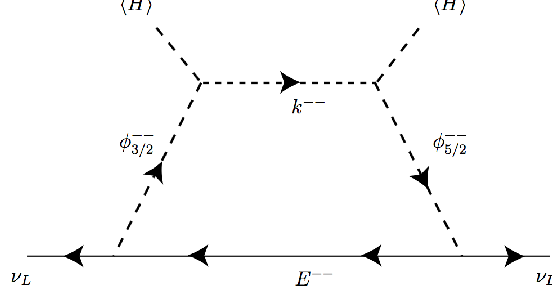


FIG. 1: One-loop diagram for generating the neutrino mass matrix.

A. Neutrino mixing

The active neutrino mass matrix M_ν is given at one-loop level via doubly-charged particles in Fig. 1, and its formula is given by

$$(M_\nu)_{ij} = \frac{2}{(4\pi)^2} \sum_{a=1}^3 f_{ia} M_{E_a} g_{aj}^T [\zeta_{12} F_I(E_a, H_1^{++}, H_2^{++}) - \zeta_{13} F_I(E_a, H_1^{++}, H_3^{++}) + \zeta_{23} F_I(E_a, H_2^{++}, H_3^{++})] \\ + (f \leftrightarrow g) \equiv f_{ia} R_a g_{aj}^T + g_{ia} R_a f_{aj}^T, \quad (\text{II.6})$$

$$F_I(a, b, c) = \frac{m_a^2 m_b^2 \ln\left(\frac{m_a}{m_b}\right) + m_a^2 m_c^2 \ln\left(\frac{m_a}{m_c}\right) + m_b^2 m_c^2 \ln\left(\frac{m_b}{m_c}\right)}{(m_a^2 - m_b^2)(m_a^2 - m_c^2)}, \quad (\text{II.7})$$

$$R_a = \frac{2M_{E_a}}{(4\pi)^2} [\zeta_{12} F_I(E_a, H_1^{++}, H_2^{++}) - \zeta_{13} F_I(E_a, H_1^{++}, H_3^{++}) + \zeta_{23} F_I(E_a, H_2^{++}, H_3^{++})], \quad (\text{II.8})$$

where $\zeta_{12} \equiv s_{12}^2 s_{13}^2 s_{23} c_{23} + 2c_{12} s_{12} s_{13} s_{23}^2 - c_{12} s_{12} s_{13} + s_{12}^2 s_{23} c_{23}$, $\zeta_{13} \equiv s_{13}^2 s_{23} c_{23}$, and $\zeta_{23} \equiv s_{23} c_{23}$. M_ν is diagonalized by the neutrino mixing matrix V_{MNS} as $M_\nu = V_{\text{MNS}} D_\nu V_{\text{MNS}}^T$ with $D_\nu \equiv \text{diag}(m_{\nu_1}, m_{\nu_2}, m_{\nu_3})$. Then one can parameterize the Yukawa coupling in terms of an arbitrary antisymmetric matrix A with complex values (i.e. $(A + A^T = 0)$) with mass scale, as follows [6, 7]:

$$f = \frac{1}{2} [V_{\text{MNS}} D_\nu V_{\text{MNS}}^T + A] (g^T)^{-1} R^{-1}, \quad g = \frac{1}{2} [V_{\text{MNS}} D_\nu V_{\text{MNS}}^T + A]^T (f^T)^{-1} R^{-1}. \quad (\text{II.9})$$

In the numerical analysis, we use *the latter* relation for convenience, and we use the data in the global analysis [8]. Notice here that the mass scale of A should be rather tiny so that A can be the relevant mass parameter to make a significant contribution to the observed neutrino oscillation data.

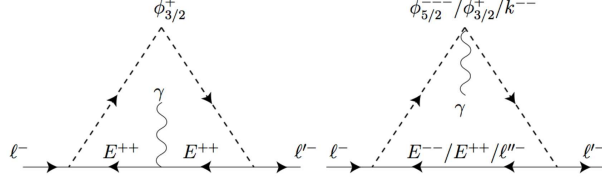


FIG. 2: One-loop diagrams for generating the lepton flavor violations, where $(g-2)_\mu$ is also induced from the same figure by sending $\ell(\ell') \rightarrow \mu$.

B. Lepton flavor violations (LFVs) and muon $g-2$

The Yukawa terms of (f, g, κ) in the Lagrangian contribute to the lepton-flavor violating processes $\ell \rightarrow \ell' \gamma$ at one-loop level as shown in Fig. 2. Here the left side of Fig. 2 arises from the term f mediated by $\phi_{3/2}^+$ and E^{++} , while the right side arises from the terms $g/f/\kappa$ that respectively correspond to $\phi_{5/2}^{--}/\phi_{3/2}^+/k^{--}$ and $E^{--}/E^{++}/\ell''^-$. The branching ratio is given by

$$B(\ell_i \rightarrow \ell_j \gamma) \approx \frac{48\pi^3 \alpha_{\text{em}}}{G_F^2} C_{ij} |\mathcal{M}_{ij}|^2, \quad (\text{II.10})$$

where $G_F \approx 1.16 \times 10^{-5} \text{ GeV}^{-2}$ is the Fermi constant, $\alpha_{\text{em}} \approx 1/137$ is the fine structure constant, $C_{21} = 1$, $C_{31} = 0.1784$, and $C_{32} = 0.1736$. $\mathcal{M}(= \mathcal{M}_f + \mathcal{M}_g + \mathcal{M}_\kappa)$ is formulated as

$$(\mathcal{M}_f)_{ij} \approx - \sum_{a=1-3} \frac{f_{ja} f_{ai}^\dagger}{(4\pi)^2} \left[F_{lfv}(E_a, \phi_{3/2}^+) + 2F_{lfv}(\phi_{3/2}^+, E_a) \right], \quad (\text{II.11})$$

$$(\mathcal{M}_g)_{ij} \approx \sum_{a=1-3} \frac{g_{ja} g_{ai}^\dagger}{(4\pi)^2} \left[3F_{lfv}(E_a, \phi_{5/2}^{++}) + 2F_{lfv}(\phi_{5/2}^{++}, E_a) \right], \quad (\text{II.12})$$

$$(\mathcal{M}_\kappa)_{ij} \approx \sum_{a,\alpha=1-3} \frac{\kappa_{ja} \kappa_{ai}^\dagger |O_{1\alpha}|^2}{3(4\pi)^2 m_{H_\alpha}^2}, \quad (\text{II.13})$$

$$F_{lvs}(a, b) = \frac{2m_a^6 + 3m_a^4 m_b^2 - 6m_a^2 m_b^4 + m_b^6 + 12m_a^4 m_b^2 \ln \left[\frac{m_b}{m_a} \right]}{12(m_a^2 - m_b^2)^4}. \quad (\text{II.14})$$

The current experimental upper bounds are given by [10, 11]

$$B(\mu \rightarrow e \gamma) \leq 4.2 \times 10^{-13}, \quad B(\tau \rightarrow \mu \gamma) \leq 4.4 \times 10^{-8}, \quad B(\tau \rightarrow e \gamma) \leq 3.3 \times 10^{-8}. \quad (\text{II.15})$$

The muon anomalous magnetic moment $(g-2)_\mu$: It is known that discrepancy of experimental value and the SM prediction is given by [12]

$$\Delta a_\mu = (26.1 \pm 8.0) \times 10^{-10}. \quad (\text{II.16})$$

We have nonvanishing $(g-2)_\mu$, and its formula is found via \mathcal{M} in LFVs as

$$\Delta a_\mu \approx -m_\mu^2 \mathcal{M}_{22}. \quad (\text{II.17})$$

Here the f term contribution provides the positive value of $(g-2)_\mu$ that corresponds to Fig. 2 with ϕ^+ and E^{++} mediators inside the loop, while the other terms g and κ give the negative values of $(g-2)_\mu$.¹ In order to achieve the agreement with the experimental value, one has to enhance f term compared to the g and κ term. However the κ term gives another LFV with three body decay $\ell_i \rightarrow \ell_j \ell_k \bar{\ell}_\ell$ at tree level and it gives more stringent constraints as shown in Table I of Ref. [9]. Thus we can expect this term to be negligible in $(g-2)_\mu$.

C. Oblique parameters

In order to estimate the testability via collider physics, we have to consider the oblique parameters that restrict the mass hierarchy between each of the components in $\Phi_{\frac{3}{2}}$ and $\Phi_{\frac{5}{2}}$.

Here we focus on the new physics contributions to S and T parameters in the case $U = 0$. Then ΔS and ΔT are defined as

$$\Delta S = 16\pi \frac{d}{dq^2} [\Pi_{33}(q^2) - \Pi_{3Q}(q^2)]|_{q^2 \rightarrow 0}, \quad \Delta T = \frac{16\pi}{s_W^2 m_Z^2} [\Pi_\pm(0) - \Pi_{33}(0)], \quad (\text{II.18})$$

where $s_W^2 \approx 0.23$ is the Weinberg angle and m_Z is the Z boson mass. The loop factors $\Pi_{33,3Q,\pm}(q^2)$ are calculated from the one-loop vacuum-polarization diagrams for Z and W^\pm

¹ The sign of $(g-2)_\mu$, which is induced at one-loop level, generally depends on sign of the electric charge and the direction of momentum of the particle that emits the photon inside the loop. For example, when a fermion (boson) with negative (positive) electric charge propagates in the same direction as the outgoing muon, one finds positive values for $(g-2)_\mu$. In the opposite case, one obtains negative $(g-2)_\mu$. Through this aspect, one can straightforwardly understand the sign of $(g-2)_\mu$ without any computations, and our sign shows the direct consequence of this insight.

bosons, which are respectively given by

$$\begin{aligned} \Pi_{33} = \frac{1}{2(4\pi)^2} & \left[G(q^2, m_{\phi_{3/2}^+}^2, m_{\phi_{3/2}^+}^2) + (|O_{2\alpha}|^2 + |O_{3\alpha}|^2) \left[G(q^2, m_{H_\alpha^{++}}^2, m_{H_\alpha^{++}}^2) - H(m_{H_\alpha^{++}}^2) \right] \right. \\ & \left. + G(q^2, m_{\phi_{5/2}^{+++}}^2, m_{\phi_{5/2}^{+++}}^2) - H(m_{\phi_{3/2}^+}^2) - H(m_{\phi_{5/2}^{+++}}^2) \right], \end{aligned} \quad (\text{II.19})$$

$$\begin{aligned} \Pi_{3Q} = \frac{1}{(4\pi)^2} & \left[-G(q^2, m_{\phi_{3/2}^+}^2, m_{\phi_{3/2}^+}^2) + 2(|O_{2\alpha}|^2 - |O_{3\alpha}|^2) \left[G(q^2, m_{H_\alpha^{++}}^2, m_{H_\alpha^{++}}^2) - H(m_{H_\alpha^{++}}^2) \right] \right. \\ & \left. + 3G(q^2, m_{\phi_{5/2}^{+++}}^2, m_{\phi_{5/2}^{+++}}^2) + H(m_{\phi_{3/2}^+}^2) - 3H(m_{\phi_{5/2}^{+++}}^2) \right], \end{aligned} \quad (\text{II.20})$$

$$\begin{aligned} \Pi_\pm = \frac{1}{2(4\pi)^2} & \left[2|O_{2\alpha}|^2 G(q^2, m_{\phi_{3/2}^+}^2, m_{H_\alpha^{++}}^2) + 2|O_{3\alpha}|^2 G(q^2, m_{\phi_{5/2}^+}^2, m_{H_\alpha^{++}}^2) \right. \\ & \left. - (|O_{2\alpha}|^2 + |O_{3\alpha}|^2) H(m_{H_\alpha^{++}}^2) - H(m_{\phi_{3/2}^+}^2) - H(m_{\phi_{5/2}^{+++}}^2) \right]. \end{aligned} \quad (\text{II.21})$$

The experimental bounds are given by [13]

$$(0.05 - 0.09) \leq \Delta S \leq (0.05 + 0.09), \quad (0.08 - 0.07) \leq \Delta T \leq (0.08 + 0.07), \quad (\text{II.22})$$

and new contributions should be within these ranges.

D. Numerical analysis

In the numerical analysis, we prepare 2×10^6 random sampling points for the relevant input parameters in the following ranges:

$$\begin{aligned} s_{12,23,13} & \in [-0.1, 0.1], \quad (A_{12}, A_{13}, A_{23}) \in \pm[10^{-18}, 10^{-8}] \text{ TeV}, \\ (f_{11}, f_{12}, f_{13}) & \in \pm[10^{-10}, 10^{-5}], \quad (f_{21}, f_{22}, f_{23}) \in \pm[1, 4\pi], \quad (f_{31}, f_{32}, f_{33}) \in \pm[10^{-3}, 1], \\ m_{H_1^{++}} & \in [0.1, 2] \text{ TeV}, \quad m_{H_2^{++}} \in [m_{H_1^{++}}, 2] \text{ TeV}, \quad m_{H_3^{++}} \in [m_{H_2^{++}}, 2] \text{ TeV}, \\ m_{\phi_{3/2}^+} & \in [m_{H_2^{++}} \pm 0.1] \text{ TeV}, \quad m_{\phi_{5/2}^{+++}} \in [m_{H_3^{++}} \pm 0.1] \text{ TeV}, \\ M_1 & \in [m_{\phi_{5/2}^{+++}}, 2] \text{ TeV}, \quad M_2 \in [M_1, 2] \text{ TeV}, \quad M_3 \in [M_2, 2] \text{ TeV}, \end{aligned} \quad (\text{II.23})$$

and we find 650 allowed points that satisfy neutrino oscillation data, LFVs, oblique parameters, and observed $(g-2)_\mu$: $\Delta a_\mu = (26.1 \pm 8.0) \times 10^{-10}$ in Eq. (II.16). Here we take rather large Yukawa couplings f_{21}, f_{22}, f_{23} in order to obtain sizable $(g-2)_\mu$. On the other hand, f_{11}, f_{12}, f_{13} have to be tiny in order to satisfy the stringent constraint of $\mu \rightarrow e\gamma$ process, which is proportional to $f_{11}f_{21} + f_{12}f_{22} + f_{13}f_{23}$, while f_{31}, f_{32}, f_{33} are taken to be of typical scale to satisfy the other LFVs.

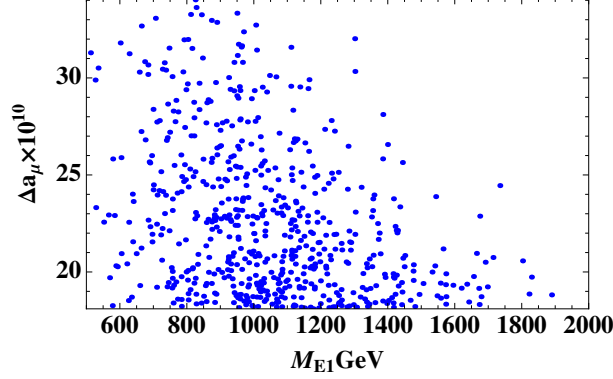


FIG. 3: Scatter plot of $\Delta a_\mu \times 10^{10}$ versus M_{E_1} GeV that satisfy all the constraints mentioned in the text.

In Fig. 3, we show the scatter plot in the plane of M_{E_1} and Δa_μ that satisfy all the constraints as discussed above. We observe that the whole mass range of E_1 that we have taken can give Δa_μ to be within $(26.1 \pm 8.0) \times 10^{-10}$. Also, the smaller the mass M_{E_1} the larger the value of Δa_μ will be, as expected by the formula in Eq. (II.11).

In Fig. 4, we show two characteristic correlations among the masses of the charged bosons. These correlations suggest that the masses between $m_{H_2^{++}} (m_{H_3^{++}})$ and $m_{\phi_{3/2}^+} (m_{\phi_{5/2}^{+++}})$ are almost degenerate. Since we have taken small mixings among the doubly-charged bosons in the input parameters, such mass degeneracy naturally occurs in each of the isospin doublets. This is a consequence of the constraint from the oblique parameters as discussed in Sec. II C. The second feature is that the mass range of $m_{\phi_{3/2}^+}$ is restricted to be less than 1 TeV, even though we have scanned it up to 2 TeV as input parameters. This mainly comes from the experimental value of Δa_μ . Moreover, the value of the loop function in (II.11) decreases when the mass of $\phi_{3/2}^+$ increases. Then $m_{H_2^{++}}$ is also restricted to be in the same range as $m_{\phi_{3/2}^+}$ by the consequence of oblique parameters again.

III. COLLIDER SIGNALS

We first consider the Drell-Yan (DY) production of $E\bar{E}$ via γ, Z exchanges. The interactions can be obtained from the kinetic term of the fermion E . Since E is a singlet, the interactions with γ and Z are given by

$$\mathcal{L} = -e\bar{E}\gamma^\mu Q_E E A_\mu + \frac{gs_W^2}{c_W}\bar{E}\gamma^\mu Q_E E Z_\mu,$$

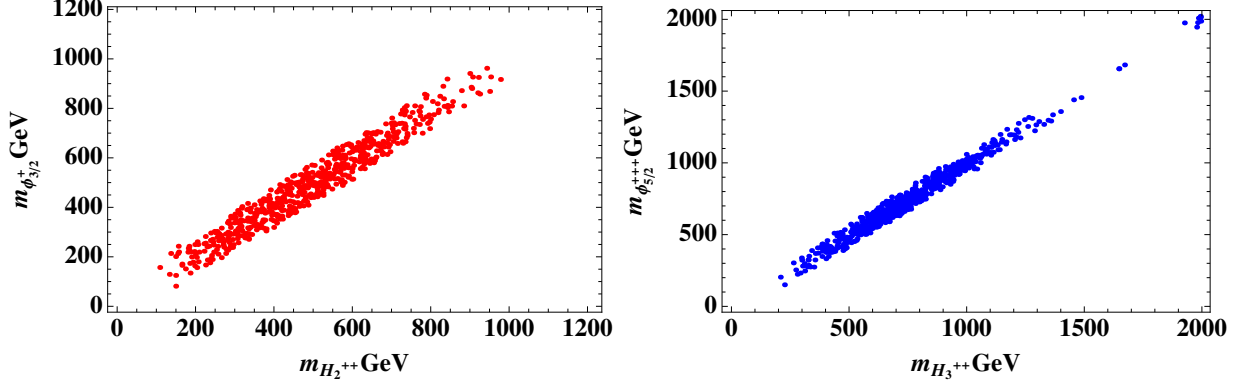


FIG. 4: Scatter plots of $m_{\phi_{3/2}^+}$ versus $m_{H_2^{++}}$ GeV with red points on the left side, and $m_{\phi_{5/2}^{++}}$ versus $m_{H_3^{++}}$ GeV with blue points on the right side. Notice here that only these two pairs have strong correlations due to the oblique parameters.

where s_W and c_W are respectively the sine and cosine of the Weinberg angle, and Q_E is the electric charge of the fermion E with $Q_E = -2$ in our model.

The square of the scattering amplitude, summed over spins, for $q(p_1)\bar{q}(p_2) \rightarrow E(k_1)\bar{E}(k_2)$ can be written as

$$\begin{aligned} \sum |\mathcal{M}|^2 &= 4e^4 Q_E^2 \left[(\hat{u} - M_E^2)^2 + (\hat{t} - M_E^2)^2 + 2\hat{s}M_E^2 \right] \\ &\times \left\{ \left| \frac{Q_q}{\hat{s}} - \frac{g_L^q}{c_W^2} \frac{1}{\hat{s} - m_Z^2} \right|^2 + \left| \frac{Q_q}{\hat{s}} - \frac{g_R^q}{c_W^2} \frac{1}{\hat{s} - m_Z^2} \right|^2 \right\}, \end{aligned} \quad (\text{III.1})$$

where \hat{s} , \hat{t} , \hat{u} are the usual Mandelstam variables for the subprocess, and $g_L^q = T_{3q} - s_W^2 Q_q$ and $g_R^q = -s_W^2 Q_q$ are the chiral couplings of quarks to the Z boson. The subprocess differential cross section is given by

$$\begin{aligned} \frac{d\hat{\sigma}}{d\cos\hat{\theta}} &= \frac{\beta e^4 Q_E^2}{96\pi} \left[(\hat{u} - M_E^2)^2 + (\hat{t} - M_E^2)^2 + 2\hat{s}M_E^2 \right] \\ &\times \left\{ \left| \frac{Q_q}{\hat{s}} - \frac{g_L^q}{c_W^2} \frac{1}{\hat{s} - m_Z^2} \right|^2 + \left| \frac{Q_q}{\hat{s}} - \frac{g_R^q}{c_W^2} \frac{1}{\hat{s} - m_Z^2} \right|^2 \right\}, \end{aligned} \quad (\text{III.2})$$

where $\beta = \sqrt{1 - 4M_E^2/\hat{s}}$, and where T_{3q} is the third component of the isospin of q . This subprocess cross section is then folded with parton distribution functions to obtain the scattering cross section at the pp collision level. The K factor for the production cross sections is expected to be similar to the conventional DY process, which is approximately $K \simeq 1.3$ at the LHC energies. The production cross sections for $pp \rightarrow E_1^{++} E_1^{--}$ at $\sqrt{s} = 13$ TeV LHC are shown in Fig. 5. For $M_{E_1} \approx 1$ TeV the cross section is about 0.2 fb.

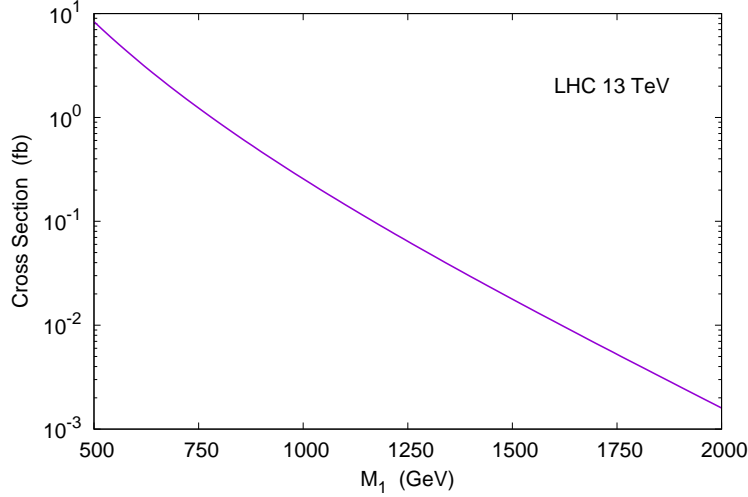


FIG. 5: Drell-Yan Production cross section for $pp \rightarrow E_1^{++} E_1^{--}$ at the LHC-13.

We proceed to estimate the decay partial widths of the fermion E_1^{--} , which is presumed to the lightest among $E_{1,2,3}^{--}$. The decay channels of E_1^{--} can proceed via the following interactions

$$\begin{aligned} \mathcal{L} = & f_{i1} \left[\bar{\nu}_i P_R E_1^{--} (O_{21} H_1^{++} + O_{22} H_2^{++} + O_{23} H_3^{++}) + \bar{e}_i P_R E_1^{--} \phi_{3/2}^+ \right] \\ & + g_{i1} \left[\bar{\nu}_i P_R E_1^c (O_{31} H_1^{--} + O_{32} H_2^{--} + O_{33} H_3^{--}) + \bar{e}_i P_R E_1^c \phi_{5/2}^{--} \right]. \end{aligned} \quad (\text{III.3})$$

We shall take the approximation that the diagonalizing matrix O is nearly diagonal, such that $O_{11}, O_{22}, O_{33} \approx 1$. In such a case, $H_1^{++} \approx k^{++}$, $H_2^{++} \approx \phi_{3/2}^{++}$ and $H_3^{++} \approx \phi_{5/2}^{++}$. We also take the simplification that the masses of each components in the doublet are similar, i.e., $m_{\phi_{3/2}^+} \approx m_{\phi_{3/2}^{++}}$ and $m_{\phi_{5/2}^{++}} \approx m_{\phi_{5/2}^{+++}}$.

We compute the partial width of $E^{--} \rightarrow e_i \phi_{3/2}^-$ and obtain

$$\Gamma(E_1^{--} \rightarrow e_i \phi_{3/2}^-) = \frac{|f_{i1}|^2}{64\pi} M_{E_1} \left(1 - \frac{m_{\phi_{3/2}}^2}{M_{E_1}^2} \right) \quad (\text{III.4})$$

which is the same as $\Gamma(E_1^{--} \rightarrow \nu_i H_2^{--})$, in which H_2^{--} is mostly $\phi_{3/2}^{--}$. Summing over all lepton and neutrino channels with $i = 1, 2, 3$ as well as the contributions from the f_{i1} and g_{i1} terms, we obtain the total decay width of E_1^{--}

$$\Gamma(E_1^{--}) = \frac{M_{E_1}}{32\pi} \left\{ \left(1 - \frac{m_{\phi_{3/2}}^2}{M_{E_1}^2} \right) \sum_{i=1}^3 |f_{i1}|^2 + \left(1 - \frac{m_{\phi_{5/2}}^2}{M_{E_1}^2} \right) \sum_{i=1}^3 |g_{i1}|^2 \right\} \quad (\text{III.5})$$

Next, we compute the subsequent decays of $H_i^{--} \rightarrow e_k^- e_l^-$ (where k, l are flavors) and $\phi_{3/2}^- \rightarrow H_i^{--} W^+$:

$$\Gamma(H_i^{--} \rightarrow e_k^- e_l^-) = \frac{\kappa_{kl}^2 |O_{1i}|^2}{16\pi} m_{H_i} \quad (\text{III.6})$$

$$\Gamma(\phi_{3/2}^- \rightarrow H_i^{--} W^+) = \frac{|O_{2i}|^2 m_{\phi_{3/2}}^3}{128\pi m_W^2} \lambda^{3/2} \left(1, \frac{m_W^2}{m_{\phi_{3/2}}^2}, \frac{m_{H_i}^2}{m_{\phi_{3/2}}^2} \right) \quad (\text{III.7})$$

where the function $\lambda(x, y, z) = (x^2 + y^2 + z^2 - 2xy - 2yz - 2zx)$ and if the mass difference $m_{\phi_{3/2}} - m_{H_i} < m_W$ then the latter decay would proceed via a virtual W boson. Here the parameter κ_{kl} can be chosen arbitrarily so as to decay the charged boson k^{--} to ensure no stable charged particles left in the Universe. Therefore, each singlet fermion E^{--} so produced can decay into 2 charged leptons or 4 charged leptons plus missing energies. In DY production of a pair of singlet fermions $E^{--} E^{++}$, the final state consists of 4 or 8 charged leptons plus missing energies, which is extremely spectacular in hadron colliders.

Similarly, the singlet fermion E_1^{--} can decay into the $\phi_{5/2}$ doublet via the second term in the Lagrangian (III.3), including $E^{--} \rightarrow \phi_{5/2}^{--} \bar{e}_i$ and $E^{--} \rightarrow H_3^{--} \bar{\nu}_i$. These partial widths have already been included in Eq. (III.5). The decay pattern of the components in the $\phi_{5/2}$ doublet is

$$\begin{aligned} (\phi_{5/2}^{--} \approx H_3^{--}) &\rightarrow e_k^- e_l^- \\ \phi_{5/2}^{--} &\rightarrow H_i^{--} W^- , \end{aligned}$$

of which their decay widths can be obtained from Eqs. (III.6) and (III.7) by replacing $m_{\phi_{3/2}} \rightarrow m_{\phi_{5/2}}$.

Naively, since $g_{i1} \ll f_{i1}$ due to lepton-number violation, we expect $E^{--} \rightarrow e_i \phi_{3/2}^-, \nu_i \phi_{3/2}^-$ dominantly. Therefore, the branching ratio for $E^{--} \rightarrow 2e_i + \cancel{E}$ is about 1/2, for $E^{--} \rightarrow 4e_i + \cancel{E}$ is about 1/6 (including $e_i = e, \mu, \tau$). Now we can estimate the event rates at the 13 TeV LHC with a luminosity of 3000 fb^{-1} (HL-LHC). We have about $0.2 \times 3000 \times (1/2)^2 = 150$ events for $4e_i$ final state, $0.2 \times 3000 \times 1/2 \times 1/6 \times 2 = 100$ events for $6e_i$ final state, and $0.2 \times 3000 \times 1/6 \times 1/6 \simeq 17$ events for $8e_i$ final state.

IV. CONCLUSIONS

In this work, we have proposed a simple extension of the SM by introducing 3 generations of doubly-charged fermion pairs and three multi-charged bosonic fields. We have investigated

the contributions of the model to neutrino mass, lepton-flavor violations, muon $g-2$, oblique parameters, and collider signals, and found a substantial fraction of the parameter space that can satisfy all the constraints.

The design of the κ term in the Lagrangian is to make sure that all new charged particles will decay into SM particles so that no stable charged particles were left in the Universe. Because of this κ term the new charged particles will decay into charged leptons in collider experiments, thus giving rise to spectacular signatures. Pair production of $E_1^{++}E_1^{--}$ can give $4e_i, 6e_i$, or $8e_i$ plus missing energies in the final state. The event rates are $17 - 150$ for an integrated luminosity of 3000 fb^{-1} .

Acknowledgments

This work was supported by the Ministry of Science and Technology of Taiwan under Grants No. MOST-105-2112-M-007-028-MY3.

-
- [1] A. Zee, Phys. Lett. B **93**, 389 (1980) [Erratum-ibid. B **95**, 461 (1980)].
 - [2] T. P. Cheng and L. F. Li, Phys. Rev. D **22**, 2860 (1980).
 - [3] A. Pilaftsis, Z. Phys. C **55**, 275 (1992) doi:10.1007/BF01482590 [hep-ph/9901206].
 - [4] E. Ma, Phys. Rev. D **73**, 077301 (2006) [hep-ph/0601225].
 - [5] M. Aoki, S. Kanemura and K. Yagyu, Phys. Lett. B **702**, 355 (2011) Erratum: [Phys. Lett. B **706**, 495 (2012)] doi:10.1016/j.physletb.2011.11.043, 10.1016/j.physletb.2011.07.017 [arXiv:1105.2075 [hep-ph]].
 - [6] H. Okada and Y. Orikasa, Phys. Rev. D **94**, no. 5, 055002 (2016) doi:10.1103/PhysRevD.94.055002 [arXiv:1512.06687 [hep-ph]].
 - [7] K. Cheung, T. Nomura and H. Okada, Phys. Rev. D **94**, no. 11, 115024 (2016) doi:10.1103/PhysRevD.94.115024 [arXiv:1610.02322 [hep-ph]].
 - [8] D. V. Forero, M. Tortola and J. W. F. Valle, Phys. Rev. D **90**, no. 9, 093006 (2014) doi:10.1103/PhysRevD.90.093006 [arXiv:1405.7540 [hep-ph]].
 - [9] J. Herrero-Garcia, M. Nebot, N. Rius and A. Santamaria, Nucl. Phys. B **885**, 542 (2014) doi:10.1016/j.nuclphysb.2014.06.001 [arXiv:1402.4491 [hep-ph]].

- [10] A. M. Baldini *et al.* [MEG Collaboration], Eur. Phys. J. C **76**, no. 8, 434 (2016)
doi:10.1140/epjc/s10052-016-4271-x [arXiv:1605.05081 [hep-ex]].
- [11] J. Adam *et al.* [MEG Collaboration], Phys. Rev. Lett. **110**, 201801 (2013)
doi:10.1103/PhysRevLett.110.201801 [arXiv:1303.0754 [hep-ex]].
- [12] K. Hagiwara, R. Liao, A. D. Martin, D. Nomura and T. Teubner, J. Phys. G **38**, 085003 (2011) doi:10.1088/0954-3899/38/8/085003 [arXiv:1105.3149 [hep-ph]].
- [13] K.A. Olive et al. (Particle Data Group), Chin. Phys. C, 38, 090001 (2014) and 2015 update.